

BI-TP 96/03
 WUE-ITP-96-001
 hep-ph/9601355

Electroweak Radiative Corrections to $e^+e^- \rightarrow W^+W^- \gamma$

A. Denner

Institut für Theoretische Physik, Universität Würzburg
 Am Hubland, D-97074 Würzburg, Germany

S. Dittmaier

Theoretische Physik, Universität Bielefeld
 Postfach 100131, D-33501 Bielefeld, Germany

R. Schuster^z

Institut für Theoretische Physik, Universität Würzburg
 Am Hubland, D-97074 Würzburg, Germany

Abstract:

We discuss the complete virtual and soft-photon $\mathcal{O}(\alpha_s)$ corrections to $e^+e^- \rightarrow W^+W^- \gamma$ within the electroweak Standard Model for arbitrary polarized photons. In the on-shell renormalization scheme for fixed M_W no leading corrections associated with the running of α or heavy top-quark and Higgs-boson masses occur. The corrections turn out to be of the order of 10%, but can become much larger where the lowest-order cross-sections are suppressed.

BI-TP 96/03
 WUE-ITP-96-001

January 1996

^yContribution to the Proceedings of the Workshop on Physics with e^+e^- Colliders, Annecy, Geneva, Hamburg, February 4 to September 1, 1995.

^zSupported by the Deutsche Forschungsgemeinschaft.

Electroweak Radiative Corrections to $e^+e^- \rightarrow W^+W^-$

A. Denner¹, S. Dittmaier² and R. Schuster^{1,y}

¹ Institut für Theoretische Physik, Universität Würzburg, Germany

² Theoretische Physik, Universität Bielefeld, Germany

1 Introduction

A particularly interesting process at e^+e^- colliders is W -pair production. Its total cross-section approaches a constant of about 80 pb at high energies corresponding to 8 $\times 10^6$ W pairs for 10 fb⁻¹. Although this large cross-section is drastically reduced by angular cuts, even for $\cos \theta < 0.8$ it is still 15 and 4 pb at a center-of-mass energy of 500 and 1000 GeV, respectively, and thus much larger as e.g. the one for $e^+e^- \rightarrow W^+W^-$. Hence $e^+e^- \rightarrow W^+W^-$ is very well-suited for precision investigations of the SM.

Most of the existing works on $e^+e^- \rightarrow W^+W^-$ concentrated on tree-level predictions and on the influence of anomalous non-Abelian gauge couplings [1, 2, 3]. At tree level, the process $e^+e^- \rightarrow W^+W^-$ depends both on the triple WWZ and the quartic $WWZZ$ coupling, and no other vertices are involved in the unitary gauge. The sensitivity to the WWZ coupling is comparable and complementary to the reactions $e^+e^- \rightarrow W^+W^-$ and $e^+e^- \rightarrow WZ$ [2]. Because the sensitivity to the WWZ coupling is much larger than the one in e^+e^- processes, $e^+e^- \rightarrow W^+W^-$ is the ideal process to study this coupling [3].

The one-loop diagrams involving a resonant Higgs boson have been calculated in order to study the possible investigation of the Higgs boson via $e^+e^- \rightarrow H \rightarrow W^+W^-$ [4, 5, 6, 7]. Based on our complete one-loop calculation [8], we have supplemented these investigations by a discussion of the heavy-Higgs effects in Ref. [9]. As a matter of fact, only the (suppressed) channels of longitudinal W -boson production are sensitive to the Higgs mechanism, but the (dominant) channels of purely transverse W -boson production are extremely insensitive. This insensitivity to the Higgs sector renders $e^+e^- \rightarrow W^+W^-$ even more suitable for the investigation of the non-Abelian self couplings.

In this paper we summarize our results for the complete virtual and soft-photonic $O(\alpha)$ corrections. We give a survey of the leading corrections and restrict the numerical

^ySupported by the Deutsche Forschungsgemeinschaft.

discussion to unpolarized W bosons. More detailed results and a discussion of their evaluation can be found in Refs. [8, 9].

2 Lowest-order cross-section

The Born cross-section of $e^+e^- \rightarrow W^+W^-$ is given by the formulae

$$\frac{d\sigma_{\text{Born}}}{d\Omega_{\text{unpol}}} = \frac{3}{2s} \left(1 - \frac{2s(2s + 3M_W^2)}{3(M_W^2 - t)(M_W^2 - u)} + \frac{2s^2(s^2 + 3M_W^4)}{3(M_W^2 - t)^2(M_W^2 - u)^2} \right) \quad (1)$$

for the unpolarized differential cross-section and

$$\sigma_{\text{Born}}^{\text{unpol}} = \frac{6}{s} \cos^2 \theta_{\text{cut}} \left(1 - \frac{4M_W^2(s - 2M_W^2)}{s^2 \cos^2 \theta_{\text{cut}}} \log \frac{1 + \cos \theta_{\text{cut}}}{1 - \cos \theta_{\text{cut}}} + \frac{16(s^2 + 3M_W^4)}{3s^2(1 - \cos^2 \theta_{\text{cut}})} \right) \quad (2)$$

for the unpolarized cross-section integrated over $\theta_{\text{cut}} < \theta < 180^\circ - \theta_{\text{cut}}$. Here $\beta = \sqrt{1 - 4M_W^2/s}$ denotes the velocity of the W bosons and s, t , and u are the usual Mandelstam variables. Concerning kinematics, polarizations, input parameters, etc., we follow the conventions of Ref. [8] throughout.

As can be seen from Table 1, the lowest-order cross-sections are dominated by transverse (T) W bosons. The massive t -channel exchange gives rise to a constant cross-section at high energies, $s \gg M_W^2$, for $\theta_{\text{cut}} = 0$

$$\sigma_{\text{UU}}^{\text{Born}} ; \sigma_{\text{UU}}^{\text{Born}}|_{s \rightarrow \infty} = \sigma_{\text{TT}}^{\text{Born}} ; \sigma_{\text{TT}}^{\text{Born}}|_{s \rightarrow \infty} = \frac{8}{M_W^2} = 80.8 \text{ pb} \quad (3)$$

For a finite cut, $\sigma_{\text{UU}}^{\text{Born}}$ and $\sigma_{\text{UU}}^{\text{Born}}$ behave as $1/s$ for large s . This is illustrated in Fig. 1 for two different angular cuts $\theta_{\text{cut}} = 10^\circ ; 20^\circ$. Close to threshold the differential and integrated cross-sections for all polarization configurations vanish like β^3 .

3 Leading corrections

Electroweak radiative corrections contain leading contributions of universal origin. In the on-shell renormalization scheme with input parameters α, M_W, M_Z these affect the corrections to $e^+e^- \rightarrow W^+W^-$ as follows:

Since the two external photons are on mass shell, the relevant effective coupling is the one at zero-momentum transfer and the running of α is not relevant.

$\sqrt{s} = \sqrt{s}$ GeV		unpol	TT	LL	TT	LL	(LT + TL)
500	0 < < 180	77.6	82.2	6.10 10^{-2}	70.2	9.99 10^{-1}	1.69
	20 < < 160	36.7	42.7	3.17 10^{-2}	28.2	9.89 10^{-1}	1.49
1000	0 < < 180	80.1	82.8	3.54 10^{-3}	76.9	2.52 10^{-1}	1.70 10^{-1}
	20 < < 160	14.2	16.8	7.18 10^{-4}	11.2	2.44 10^{-1}	1.21 10^{-1}
2000	0 < < 180	80.6	81.6	2.14 10^{-4}	79.5	6.41 10^{-2}	1.50 10^{-2}
	20 < < 160	4.07	4.84	1.27 10^{-5}	3.23	6.11 10^{-2}	8.26 10^{-3}

Table 1: Lowest-order integrated cross-sections in pb for several polarizations; the lowest-order cross-section for (LT + TL) vanishes.

In order to handle the Higgs-boson resonance at $s = M_H^2$, in the literature [5, 6, 7] the Higgs-boson width has been introduced naively by the replacement

$$\frac{F^H(s)}{s - M_H^2} \rightarrow \frac{F^H(s)}{s - M_H^2 + i M_H \Gamma_H} \quad (4)$$

in the resonant contribution. However, this treatment destroys gauge invariance at the level of non-resonant $O(\Gamma)$ corrections. In order to preserve gauge invariance, we decompose the Higgs-resonance contribution into a gauge-invariant resonant part and a gauge-dependent non-resonant part and introduce Γ_H only in the former:

$$\frac{F^H(s)}{s - M_H^2} \rightarrow \frac{F^H(M_H^2)}{s - M_H^2 + i M_H \Gamma_H} + \frac{F^H(s) - F^H(M_H^2)}{s - M_H^2} : \quad (5)$$

Outside the region of Higgs resonance the Higgs-mass dependence is small for unpolarized W bosons. For all polarizations no corrections involving $\log(M_H/M_W)$ or M_H^2/M_W^2 arise in the heavy-Higgs limit [9]. However, for $\sqrt{s} \sim M_H \sim M_W$ corrections proportional to M_H^2/M_W^2 appear for the cross-sections involving longitudinal (L) gauge bosons as a remnant of the unitarity cancellations. These terms give rise to large effects in particular for cross-sections with longitudinal W bosons.

The top-mass-dependent corrections are also small and behave similar to the Higgs-mass-dependent corrections for $\sqrt{s} \sim m_t \sim M_W$; more precisely neither corrections proportional to m_t^2 nor proportional to $\log m_t$ occur in this limit for fixed M_W .

As W^+W^- involves no light charged external particles, no large logarithmic corrections associated with collinear photons show up (apart from the region of very high energies, $s \gg M_W^2$). As a consequence, the photonic corrections are not enhanced with respect to the weak corrections.

Close to threshold, i.e. for $\sqrt{s} \approx 2M_W$, the Coulomb singularity gives rise to the large universal correction

$$\delta_{\text{Coul}} = \frac{\pi}{2} \frac{v}{\sqrt{s}} \delta_{\text{Born}} : \quad (6)$$

The factor $\frac{v}{\sqrt{s}}$ is typical for the pair production of stable (on-shell) particles. For the generalization to unstable (off-shell) particles see Ref. [10].

At high energies, $\sqrt{s} \gg M_W^2$, the radiative corrections are dominated by terms like $(\frac{v}{\sqrt{s}})^2 \log^2(\sqrt{s}/M_W)$, which arise from vertex and box diagrams. At 1 TeV these are about 10%, setting the scale for the (weak) radiative corrections at this energy.

4 Numerical results

Electromagnetic and genuine weak corrections cannot be separated in a gauge-invariant way on the basis of Feynman diagrams. As no leading collinear logarithms occur in W^+W^- , the only source of enhanced photonic corrections are the soft-photon-cut-off-dependent terms which yield the relative correction

$$\delta_{\text{cut}} = \frac{2}{\sqrt{s}} \log \frac{E}{E_{\text{cut}}} \left(1 - \frac{s - 2M_W^2}{s} \log \frac{1 + \sqrt{1 - 4M_W^2/s}}{1 - \sqrt{1 - 4M_W^2/s}} \right) : \quad (7)$$

Since we are mainly interested in the weak corrections, we discard the (gauge-invariant) cut-off-dependent terms (7) by setting the soft-photon cut-off energy E_{cut} equal to the beam energy E and consider the rest as a suitable measure of the weak corrections. If not stated otherwise, the correction stands in the following for the complete relative soft-photonic and virtual electroweak corrections with $E_{\text{cut}} = E$.

Figure 1 shows the "weak" corrections to the total cross-sections integrated over 10, 170 and 20 GeV for unpolarized W bosons. The corrections for different photon polarizations almost coincide with each other and reach roughly 20% for $\sqrt{s} = 10$ and 35% for $\sqrt{s} = 20$ at $\sqrt{s} = 2$ TeV. At low energies the cross-sections with equal photon and W boson helicities are dominated by the Higgs resonance. Note that owing to helicity conservation the other cross-sections are not affected by the Higgs resonance.

In Table 2 we list the unpolarized cross-sections and the corresponding corrections for several energies and scattering angles. We include the corrections for a soft-photon-energy cut-off $E_{\text{cut}} = 0.1E$, i.e. the cut-off-dependent corrections δ_{cut} from (7), and the individual (gauge-invariant) fermionic δ_{ferm} and bosonic corrections δ_{bos} . The fermionic corrections consist of all loop diagrams and counterterm contributions involving fermion loops, all

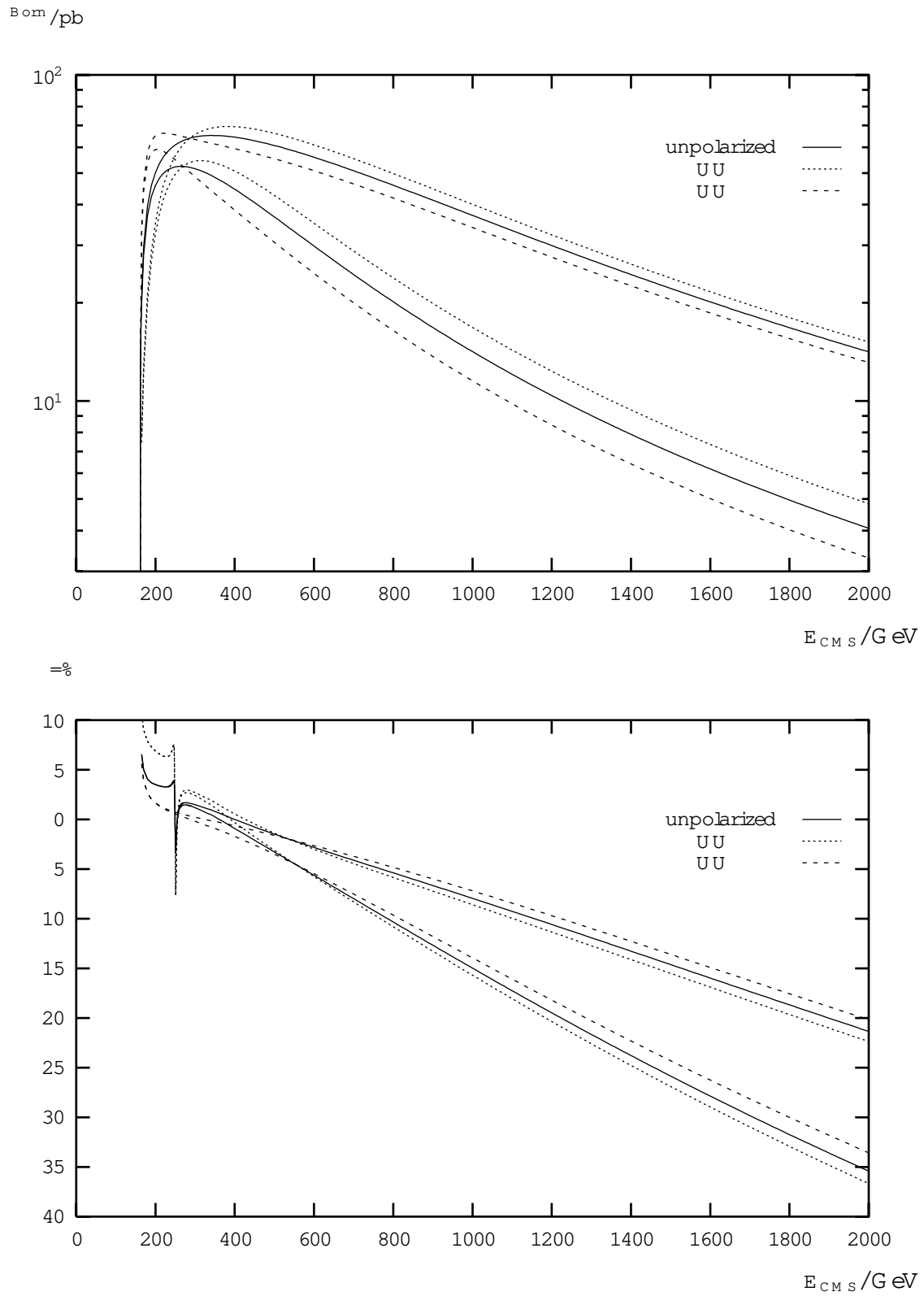


Figure 1: Integrated lowest-order cross-sections and corresponding relative corrections for an angular cut 10 170 (upper set of curves in each plot) and 20 160 (lower set).

$\sqrt{s} = \text{GeV}$		$\sigma_{\text{Boson}} = \text{pb}$	$E = 0.1E = \%$	$\text{cut} = \%$	$E = E = \%$	$\sigma_{\text{bos}} = \%$	$\sigma_{\text{ferm}} = \%$
500	5	98.13	0.02	2.79	2.81	1.49	1.32
	20	26.04	2.68	2.79	0.11	0.08	0.19
	90	0.724	10.79	2.79	8.00	5.62	2.38
	0 < < 180	77.55	3.38	2.79	0.59	0.65	0.06
	10 < < 170	60.74	4.27	2.79	1.48	1.21	0.27
	20 < < 160	36.67	6.06	2.79	3.27	2.39	0.89
1000	5	291.9	2.06	4.31	2.25	1.04	1.21
	20	15.61	11.90	4.31	7.59	6.37	1.22
	90	0.193	31.64	4.31	27.33	21.93	5.40
	0 < < 180	80.05	7.08	4.31	2.77	2.71	0.06
	10 < < 170	37.06	12.26	4.31	7.95	6.65	1.30
	20 < < 160	14.16	19.29	4.31	14.98	12.20	2.78
2000	5	418.8	7.14	5.80	1.33	1.59	0.25
	20	5.163	30.31	5.80	24.51	20.96	3.55
	90	0.049	59.59	5.80	53.78	45.47	8.32
	0 < < 180	80.59	9.85	5.80	4.04	3.95	0.09
	10 < < 170	14.14	27.15	5.80	21.35	18.34	3.01
	20 < < 160	4.068	41.22	5.80	35.41	30.12	5.29

Table 2: Lowest-order cross-sections and relative corrections for unpolarized particles

other contributions from the bosonic corrections. The fermionic corrections stay below 5% even for high energies. The bosonic contributions are responsible for the large corrections at high energies, in particular in the central angular region.

In Ref. [2] the total cross-section and the ratios

$$R_{\text{ID}} = \frac{(\sigma_{\text{os}} \text{ } j < 0.4)}{(\sigma_{\text{os}} \text{ } j < 0.8)}; \quad R_{\text{LT}} = \frac{\sigma_{\text{LL}}}{\sigma_{\text{TT}}}; \quad R_{02} = \frac{\sigma_{++}}{\sigma_{+}}; \quad (8)$$

have been investigated in view of their sensitivity to anomalous couplings.¹ We list the lowest-order predictions together with the $\mathcal{O}(\alpha_s)$ -corrected ones and the relative "weak" corrections for these observables in Table 3 using $\sigma_{\text{cut}} = 0.8$.

In Fig. 2 we plot the integrated cross-section including $\mathcal{O}(\alpha_s)$ "weak" corrections using $\sigma_{\text{cut}} = 20$ for various values of the Higgs-boson mass. While the Higgs resonance is comparably sharp for small Higgs-boson masses, it is washed out by the large width of the Higgs boson for high M_H . Already for $M_H = 400 \text{ GeV}$ the Higgs resonance is hardly visible.

¹Note that we do not perform a convolution with a realistic photon spectrum but consider the incoming photons as monochromatic.

\sqrt{s} / GeV		σ / pb	R_{LO}	R_{LT}	R_{O2}
500	Born level	15.74	0.265	0.0308	1.934
	corrected	14.82	0.259	0.0325	1.950
	corrections %	5.83	2.02	5.43	0.78
1000	Born level	4.659	0.241	0.0235	2.229
	corrected	3.617	0.227	0.0276	2.184
	corrections %	22.36	5.64	17.08	2.05
2000	Born level	1.218	0.234	0.0220	2.307
	corrected	0.647	0.207	0.0321	2.168
	corrections %	46.86	11.53	46.11	6.02

Table 3: Tree-level and $\mathcal{O}(\alpha_s)$ results for various observables using $p_{\text{cut}} = 0.3$

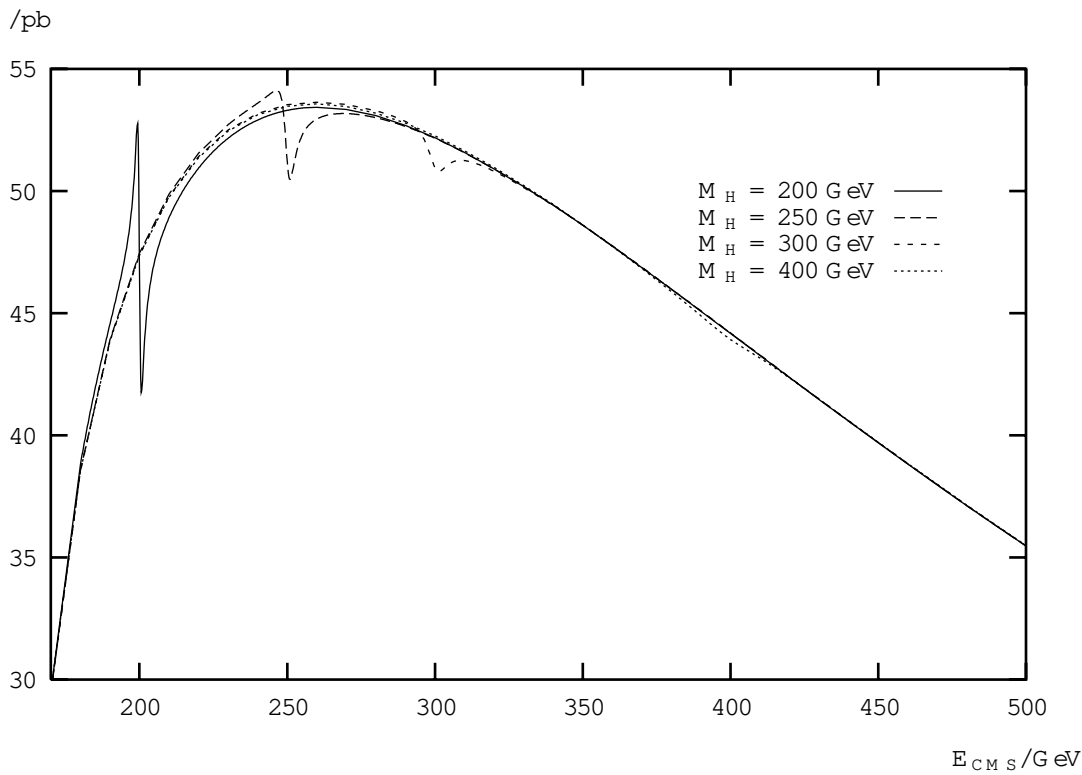


Figure 2: Integrated unpolarized cross-section including $\mathcal{O}(\alpha_s)$ "weak" corrections for various Higgs-boson masses ($20 < \sqrt{s} < 160$)

5 Summary

The process $e^+e^- \rightarrow W^+W^-$ will be one of the most interesting reactions at future colliders. In particular, it is very useful to study non-Abelian gauge couplings.

We have calculated the one-loop radiative corrections to $e^+e^- \rightarrow W^+W^-$ within the electroweak Standard Model in the soft-photon approximation for arbitrary polarizations of the photons and W bosons. An interesting peculiarity of $e^+e^- \rightarrow W^+W^-$ is the absence of most universal leading corrections, such as the running of α and leading logarithms associated with collinear bremsstrahlung. Therefore, theoretical predictions are very clean. The variation of the cross-sections with the top-quark and Higgs-boson masses is small if M_W is kept fixed with the exception of the cross-sections involving longitudinal W bosons at high energies. In the heavy mass limit no leading m_t^2 , $\log m_t$, and $\log M_H$ terms exist.

The soft-photon-cut-off-independent radiative corrections to the total cross-section are of the order of 10% and can reach up to 50% at 2 TeV. The large corrections are due to bosonic loop diagrams whereas the effects of the fermionic ones are of the order of 5(10%.

References

- [1] K.J. Kin and Y.S. Tsai, Phys. Rev. D 8 (1973) 3109;
G. Tupper and M.A. Samuel, Phys. Rev. D 23 (1981) 1933;
S.Y. Choi and F. Schrempp, Phys. Lett. B 272 (1991) 149.
- [2] E. Yehudai, Phys. Rev. D 44 (1991) 3434.
- [3] G. Belanger and F. Boudjema, Phys. Lett. B 288 (1992) 210.
- [4] M.A. Shifman et al., Sov. J. Nucl. Phys. 30 (1979) 711.
- [5] E.E. Boos and G.V. Jikia, Phys. Lett. B 275 (1992) 164.
- [6] D.A. Morris, T.N. Truong and D. Zappala, Phys. Lett. B 323 (1994) 421.
- [7] H. Veltman, Z. Phys. C 62 (1994) 235.
- [8] A. Denner, S. Dittmaier and R. Schuster, Nucl. Phys. 452 (1995) 80.
- [9] A. Denner, S. Dittmaier and R. Schuster, Phys. Rev. D 51 (1995) 4738.
- [10] V.S. Fadin, V.A. Khoze and A.D. Martin, Phys. Lett. B 311 (1993) 311; Phys. Rev. D 52 (1995) 1377;
D. Bardin, W. Beenakker and A. Denner, Phys. Lett. B 317 (1994) 213.